

## Article

# Splicing variant of AIMP2 as an effective target against chemoresistant ovarian cancer

Jin Woo Choi<sup>1,2,†</sup>, Jeong-Won Lee<sup>3,†</sup>, Jun Ki Kim<sup>2</sup>, Hye-Kyung Jeon<sup>3</sup>, Jung-Joo Choi<sup>3</sup>, Dae Gyu Kim<sup>1</sup>, Byoung-Gie Kim<sup>3</sup>, Do-Hyun Nam<sup>4</sup>, Hong Joong Kim<sup>5</sup>, Seok Hyun Yun<sup>2</sup>, and Sunghoon Kim<sup>1,6,\*</sup>

<sup>1</sup> Medicinal Bioconvergence Research Center, Advanced Institutes of Convergence Technology, Suwon, Gyeonggi 443-759, Korea

<sup>2</sup> Wellman Center for Photomedicine, Massachusetts General Hospital, Harvard Medical School, Boston, MA 02114, USA

<sup>3</sup> Department of Obstetrics and Gynecology, Samsung Medical Center and Samsung Biomedical Research Institute, Sungkyunkwan University School of Medicine, Seoul 135-710, Korea

<sup>4</sup> Department of Neurosurgery, Samsung Medical Center and Samsung Biomedical Research Institute, Sungkyunkwan University School of Medicine, Seoul 135-710, Korea

<sup>5</sup> Neomics Co., Ltd., Suwon, Gyeonggi 443-759, Korea

<sup>6</sup> WCU Department of Molecular Medicine and Biopharmaceutical Sciences, Seoul National University, Seoul 151-742, Korea

<sup>†</sup> These authors contributed equally to this work.

\* Correspondence to: Sunghoon Kim, E-mail: sungkim@snu.ac.kr

**Chemoresistance is a main cause for the failure of cancer management and intensive investigation is on-going to control chemoresistant (CR) cancers. Although NF- $\kappa$ B has been suggested as one of the potential targets to alleviate chemoresistance of epithelial ovarian cancer (EOC), direct targeting of NF- $\kappa$ B may result in an unexpected effect due to the complex regulatory network via NF- $\kappa$ B. Here we show that AIMP2-DX2, a splicing variant of tumor suppressor AIMP2, can be a therapeutic target to control CR EOC. AIMP2-DX2 was often highly expressed in CR EOC both *in vitro* and *in vivo*. AIMP2-DX2 compromised the tumor necrosis factor alpha-dependent pro-apoptotic activity of AIMP2 via the competitive inhibition of AIMP2 binding to TRAF2 that plays a pivotal role in the regulation of NF- $\kappa$ B. The direct delivery of siRNA against AIMP2-DX2 into abdominal metastatic tumors of ovarian cancer using a microneedle converged on microendoscopy significantly suppressed the growth rate of tumors. The treated cancer tissues showed an enhanced apoptosis and the decreased TRAF2 level. Thus, we suggest that the downregulation of AIMP2-DX2 can be a potent adjuvant therapeutic approach for CR EOC that resulted from an aberrant activity of NF- $\kappa$ B.**

**Keywords:** multi-tRNA synthetase complex, AIMP2, splicing variant, ovarian cancer, chemoresistant cancer, NF- $\kappa$ B

## Introduction

Ovarian carcinoma is the leading cause of death among patients with gynecological cancers. Chemoresistance is the primary factor limiting the success of long-term treatment in patients with ovarian carcinoma. Even if the tumor initially responds to chemotherapy, most patients experience drug resistance over the course of treatment, eventually leading to the recurrence of tumor and death at the late stage. To overcome the chemoresistance, many molecular candidates have been studied as potential therapeutic target. Among them, NF- $\kappa$ B is one of the most prominent molecules considered as the cause and the result of drug resistance (Nakanishi and Toi, 2005; Chen et al., 2007). Chemotherapy induces the NF- $\kappa$ B activity through the effect of p53 in response to DNA damage (Janssens et al., 2005) and the activity of NF- $\kappa$ B is kept high until the late stage of the treatment. As NF- $\kappa$ B is a

transcription factor to induce many cancer-related genes, a high level of NF- $\kappa$ B induced by chemotherapy would render tumor cells favorable for their survival (Karin, 2006).

Tumor necrosis factor alpha (TNF- $\alpha$ ) is a potent activator of NF- $\kappa$ B in various disease conditions including cancer (Balkwill, 2006; Sethi et al., 2009). Although TNF- $\alpha$  can function as a pro-apoptotic signal in some immune cells, it induces proliferation in most of the epithelial cells (Hsu et al., 1996; Micheau and Tschopp, 2003). Thus, TNF- $\alpha$  is suggested as a critical factor in disease progression and a cause for poor prognosis in several kinds of cancer including ovarian cancer (Liu et al., 2006; Charles et al., 2009; Dobrzycka et al., 2009; Kwong et al., 2009; Hernandez et al., 2010). Since the activity of NF- $\kappa$ B determines the outcome by TNF- $\alpha$  (Liu, 2005), a TNF- $\alpha$ -induced cellular proliferative function is at least partly due to NF- $\kappa$ B that is abnormally induced in chemoresistant (CR) ovarian cancer.

AIMP2, a component of multi-tRNA synthetase complex (MSC), was recently reported as a potent tumor suppressor working through multiple signaling pathways (Choi et al., 2009b). It suppresses cellular proliferation upon TGF- $\beta$  (Kim et al., 2003), and

also induces cell death under a DNA damaging condition through the protection of p53 from the attack of MDM2 (Han et al., 2008). Interestingly, AIMP2-DX2, lacking the second exon among the total of four exons encoding the full-length AIMP2, is induced during tumorigenesis (Choi et al., 2011). AIMP2-DX2 compromises the tumor suppressive activity of AIMP2-F (full-length) through the competitive binding to p53 (Han et al., 2008). While both AIMP2-F and -DX2 bind p53 with similar affinity, AIMP2-DX2 cannot protect p53 from MDM2-mediated degradation of p53.

AIMP2-F also suppresses NF- $\kappa$ B under TNF- $\alpha$  (Choi et al., 2009a). AIMP2 mediates pro-apoptotic activity of TNF- $\alpha$  via the ubiquitin-dependent degradation of TRAF2, a critical regulator of TNF- $\alpha$  signaling. AIMP2 facilitates the association of c-IAP1, E3 ubiquitin ligase with TRAF2 through trimeric interactions. As AIMP2-DX2 worked as an antagonist against AIMP2-F on p53 activation, AIMP2-DX2 may exert the opposing effect on the role of AIMP2-F in TNF- $\alpha$ -induced NF- $\kappa$ B signaling. In this work, we investigate whether AIMP2-DX2 is also implicated in the pro-apoptotic role of AIMP2-F in TNF- $\alpha$  signaling pathway, and whether it can be an effective target that can overcome the chemoresistance of ovarian cancer.

## Results

### Increased level of AIMP2-DX2 in CR ovarian cancer

As AIMP2 is a tumor suppressor in a few different cancer models (Choi et al., 2009b) and its oncogenic variant AIMP2-DX2 reflects

cancer progression and survival (Choi et al., 2011), here we investigated whether the expression of this variant in ovarian cancer has any pathological implication in ovarian cancer because ovarian cancer is a representative refractory and incurable disease once it becomes CR after multiple dosages of platinum-based combination chemotherapy (McGuire et al., 1996; Sood and Buller, 1998; Eltabbakh, 2004).

As the first step, we collected frozen samples from 40 tumor and 11 normal regions to determine the expression levels of AIMP2-F and -DX2 by real-time RT-PCR (Supplementary Table S1). The experimental procedure was guided by the protocol of the institutional review board. While the expression of AIMP2-F was not significantly changed in tumor tissues (Figure 1A, left panel), the AIMP2-DX2 expression level and the ratio of AIMP2-DX2 to -F were increased in tumor tissues (Figure 1A, middle and right panels). We then investigated whether the increased expression of AIMP2-DX2 would show any positive correlation with a particular condition of ovarian cancer. Among several kinds of factors including FIGO stage, histologic type, tumor grade, recurrence, survival, and chemosensitivity that were validated statistically, the raised expression of AIMP2-DX2 was prominently correlated with the CR property of cancer (Supplementary Table S1 and Figure 1B). When we analyzed it with the Cp value for total patients, the expression of AIMP2-F was little changed in the CR samples and AIMP2-DX2 also appeared to be expressed stably (Figure 1B, left and middle panels); while the ratio of AIMP2-DX2 to -F was obviously mounted up in CR tissues when the values

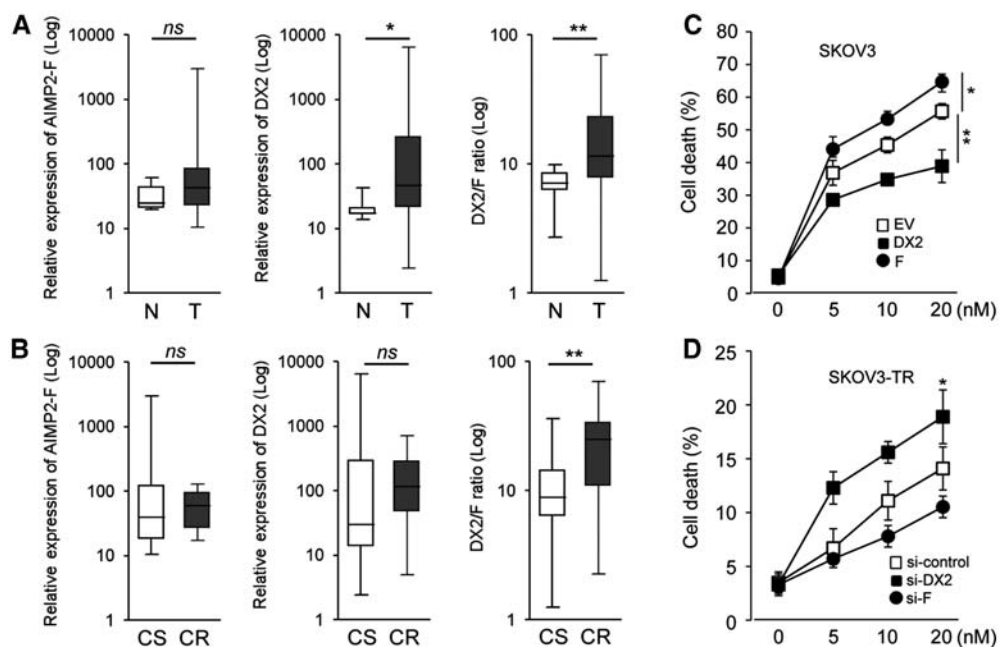


**Figure 1** Increased expression of AIMP2-DX2 in CR ovarian cancer. (A) The expression level of AIMP2-F and -DX2 was tested by real-time PCR with the specific primers and probes. The expression of AIMP2-F was not much different between the normal and tumor regions (left). AIMP2-DX2 showed a significant induction in the tumor tissues (middle). The expression ratio of AIMP2-DX2 to -F was calculated based on the results from left two graphs (right). ns, not significant. \* $P < 0.05$ , \*\* $P < 0.01$ . (B) The samples were classified by category of chemosensitivity. Fourteen CR samples showed an increased ratio of AIMP2-DX2 to -F when significantly compared with 26 CS ones (right). The individual expression of AIMP2-F and -DX2 was not enhanced in CR (left,  $P = 0.4439$  and middle,  $P = 0.1781$ ). ns, not significant. \*\* $P < 0.01$ . (C) AIMP2-F, -DX2 or pCDNA 3 (EV) were transfected into SKOV3 cells. After 24 h from the transfection, paclitaxel was treated on those cells for another 24 h at the indicated doses and the experiment was repeated three times independently. \* $P < 0.05$ , \*\* $P < 0.01$ . (D) si-RNA against AIMP2-F or DX2 was introduced into SKOV3-TR cells. After 48 h, the cells were incubated with paclitaxel for 24 h as above. \* $P < 0.05$ .

were calculated for each patient (Figure 1B, right panel, and Supplementary Table S1). To confirm if the observation obtained from the clinical specimen is reproduced *in vitro*, the expression of AIMP2-DX2 variant was further checked *in vitro* with CR pairs derived from chemosensitive (CS) ovarian cancer cell lines. A2780-CP20 is a cisplatin-resistant cell line originating from A2780-PAR. SKOV3-TR and HeyA8-MDR are commonly taxane resistant and derived from SKOV3 and HeyA8, respectively. When we tested the expression of AIMP2-F and -DX2 in all the tested cell line pairs, the expression ratio of AIMP2-DX2 to -F was significantly increased in CR cells (Supplementary Figure S1A). Next, we determined the protein levels of AIMP2-F and -DX2 that are not bound to MSC since these free forms of two proteins are the portion that is actually involved in TNF signaling pathway (Choi et al, 2011). To monitor the free forms of AIMP2-F and -DX2, the supernatant was subjected to western blot after pulling down the MSC portion from the whole cell lysates by using antibody against the complex component AIMP1. Western blot showed that AIMP2-DX2 was increased in CR cells compared with CS cells (Supplementary Figure S1B). To check whether AIMP2-DX2 could result in chemoresistance, we transfected AIMP2-F, -DX2, or pcDNA3 empty vector into SKOV3 cells and then treated them with paclitaxel in a dose-dependent manner. The increased expression of AIMP2-F and -DX2 was confirmed by PCR (Supplementary Figure S2, left panel). Whereas AIMP2-F led cells more vulnerable to apoptosis, AIMP2-DX2 compromised the apoptotic activity of the chemical (Figure 1C). To confirm whether the downregulation of AIMP2-DX2 can obtund chemoresistance, we introduced siRNA against AIMP2-F or -DX2 into SKOV3-TR cells. The expression of AIMP2-F and -DX2 appeared to be prominently decreased (Supplementary Figure S2, right panel). As SKOV3-TR has a CR property, we could just see a small population (11.2%) of cell death even at the high dose of the chemical with si-control-introduced cells. However, when AIMP2-DX2 was suppressed, the CS property on paclitaxel was partly recovered up to 18.9% (Figure 1D).

#### *Effect of AIMP2-DX2 on NF- $\kappa$ B activity*

We previously showed that AIMP2 can mediate pro-apoptotic activities of p53 (Han et al., 2008) and NF- $\kappa$ B pathways (Choi et al., 2009a), both of which are implicated for chemoresistance of cancer cells. However, ovarian cancer cells such as SKOV3 and A2780 already have inactivating mutations in p53 loci and their contribution to UV-induced apoptosis was not significantly different between CS and CR cells (Supplementary Figure S3A and B). On the other hand, CR cells showed higher resistance to TNF- $\alpha$ /cycloheximide-induced cell death (Supplementary Figure S4A and B). Both the CS and CR cell lines showed similar levels of TNF receptors I and II, suggesting that the difference in the response to TNF-induced cell death did not result from the expression change in the TNF receptors (Supplementary Figure S5A and B).

Taken together, it was plausible to explain that the effect of AIMP2-DX2 on CR EOC was weighted toward the NF- $\kappa$ B pathway rather than p53. To prove this, we explored how AIMP2-DX2 would affect the NF- $\kappa$ B activation. As NF- $\kappa$ B enhances cellular survival and proliferation, we examined the change in the cellular growth rate according to the expression level of AIMP2-DX2 in

the presence or absence of TNF- $\alpha$ , the most potent activator for NF- $\kappa$ B. While the growth of EV-transfected SKOV3 was to be faster under TNF- $\alpha$ , up to 9.9%, compared with the condition without TNF- $\alpha$  (Figure 2A), the growth rate of AIMP2-DX2-overexpressed SKOV3 was mounted up by 27.4% upon TNF- $\alpha$ . The increased expression of AIMP2-F and -DX2 was sustained until 5 days after the introduction of vectors (Supplementary Figure S6, left panel). Reversely, when we restrained the expression of AIMP2-DX2 using siRNA, the cellular growth rate was decreased by 16.1% under TNF- $\alpha$  compared with the normal culture condition (Figure 2B). We confirmed the suppressive effect of siRNAs on the target transcripts in the cell extracts obtained after 5 days of incubation (Supplementary Figure S6, right panel).

Next we investigated how the expression of AIMP2-F and -DX2 would influence the NF- $\kappa$ B activity and TNF- $\alpha$ -induced cell death in ovarian cells. We established cell lines containing different expression levels of AIMP2-F and -DX2 using SKOV3 cells that contain the inactive p53 to rule out the effect of p53 on cell death (Figure 2C). As the increased NF- $\kappa$ B activity suppressed pro-apoptotic signal of TNF- $\alpha$ , the effect of AIMP2-F and -DX2 on the NF- $\kappa$ B activity was monitored by luciferase assay. As expected, AIMP2-DX2 increased the NF- $\kappa$ B activity, whereas AIMP2-F gave the opposite effect (Figure 2D). The cell death in response to TNF- $\alpha$  was increased according to the expression level of AIMP2-F but reversely correlated with the expression levels of AIMP2-DX2 (Figure 2E). We further investigated the effect of the two forms of AIMP2 on TNF- $\alpha$  signaling pathway by measuring the cell death and NF- $\kappa$ B activity after knockdown of either AIMP2-F or -DX2 (Figure 2F). We suppressed the expression of AIMP2-F or -DX2 with the specific siRNAs and compared their effect in apoptotic response to TNF- $\alpha$ . In this case, the cell death was reduced by the suppression of AIMP2-F while mounted up when AIMP2-DX2 was suppressed (Figure 2F, left panel). Conversely, the NF- $\kappa$ B activity was enhanced and reduced by the suppression of AIMP2-F and -DX2, respectively (Figure 2F, right panel). Combined together, these results demonstrate the antagonistic function of AIMP2-DX2 against AIMP2-F in apoptotic response to TNF- $\alpha$ .

#### *AIMP2-DX2 as an effective target against CR ovarian cancer*

The increased level of AIMP2-DX2 in CR cancer cells suggest that it may be required for the survival of cancer cells in response to cytotoxic stress induced by drugs. If this is the case, the suppression of AIMP2-DX2 may restore or enhance the susceptibility to the drugs to which cancer cells have acquired resistance. To test this possibility, we designed an animal model in which we can monitor the effect of AIMP2-DX2 suppression on tumor growth. Both the CR types of A2780 and SKOV3 cells were injected into the abdomen of nude mice to mimic metastasis of human ovarian cancer.

For image-guided therapy in abdomen, we employed microneedle in laparoscopy at the end of the endoscope for direct microinjection into cancer region (Figure 3A). The endoscope of 1.9 mm diameter and microneedle of 31G were combined in the sheath of 2.5 mm diameter. The device enabled us to observe the inside of abdomen and manipulate metastasized tumor repeatedly for a few months with an incision of only 5 mm on the abdomen. We selected the remote and well-attached tumors to

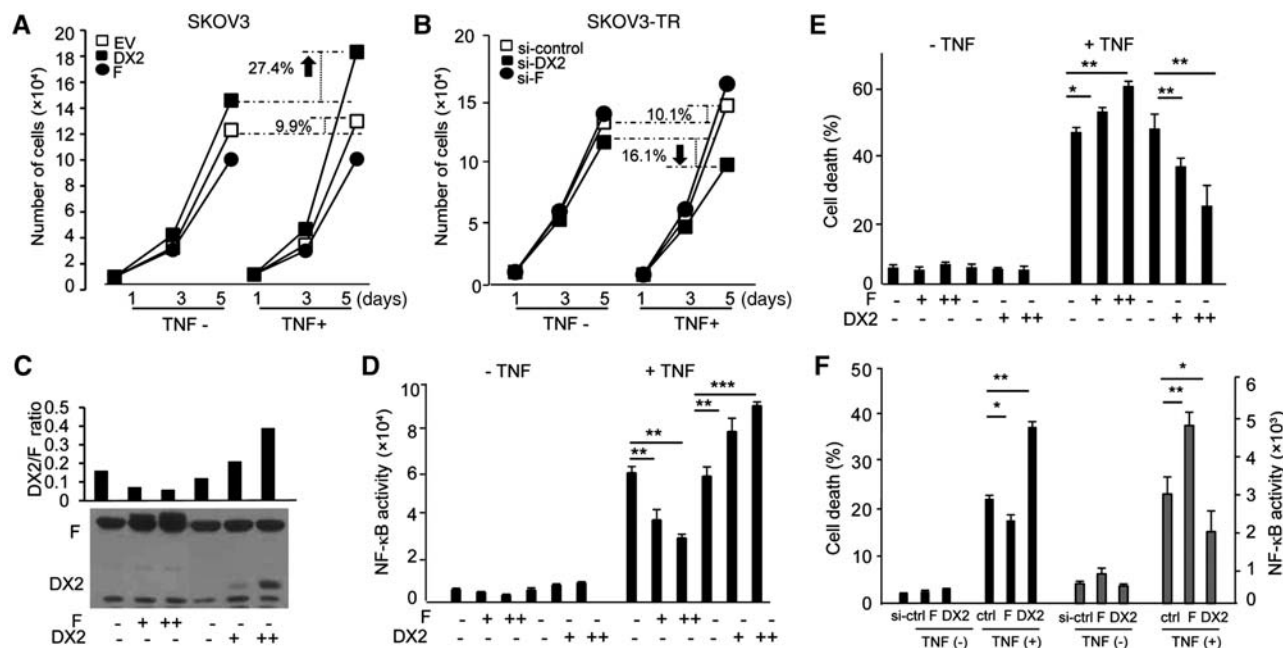


**Figure 2** AIMP2-DX2 induces cell survival through NF-κB signaling. **(A)** Three micrograms of vector DNA was transfected into 35 mm dish with lipofectamine 2000. After 12 h, the number of SKOV3 cells transfected with AIMP2-F or -DX2 was counted for 5 days in the presence or absence of TNF-α. EV-transfected cells were used as a control. The number of AIMP2-DX2-introduced cells was increased rapidly compared with that in the culture condition without TNF-α. **(B)** siRNA against AIMP2-F or -DX2 was introduced into CR SKOV3-TR. siRNA scramble was used as the control. After 24 h from the introduction, the cell numbers were counted for 5 days and the results were compared among the three groups. In the case where si-AIMP2-DX2 was transfected, the cells grew more slowly compared with control cells. **(C)** pCDNA3 vector or the vectors coding AIMP2-F or -DX2 at the two different doses were transfected into 30 mm dish of SKOV3 and then the cells were selected under G418 (1 mg/ml). After 2 weeks, cells survived were collected and the whole cell lysates from them were assessed with western blotting by using the monoclonal antibody for AIMP2-DX2. The ratio of AIMP2-DX2 to -F was measured by densitometry. **(D)** The NF-κB activity upon TNF-α was tested with cells containing various ratios of AIMP2-DX2 to -F by using the 3× NF-κB-Luc vector. TNF-α (20 ng/ml) was treated without cycloheximide for 12 h.  $^{*}P < 0.01$ ,  $^{***}P < 0.001$ . **(E)** Cell death upon TNF-α was tested with cells containing different ratios of AIMP2-DX2 to -F. Apoptotic population was calculated by FACS.  $^{*}P < 0.05$ ,  $^{**}P < 0.01$ . **(F)** The effect of downregulation of AIMP2-F or -DX2 with their siRNAs was also monitored with cell death in SKOV3 cells (left panel). The effect on TNF-α-induced NF-κB activation was compared with each other as above (right panel).  $^{*}P < 0.05$ ,  $^{**}P < 0.01$ .

follow-up without an error and to stably inject siRNA. The location of a single tumor could be confirmed by measuring the distance and direction from the incision and by comparing the structure of tissues around the tumor with previous one. Once the tumors were found, their volumes were calculated and anti-DX2-siRNA was introduced into two sites of a tumor at the interval of 3 days by microneedle. The siRNA of 50 μg was injected in the volume of 10 μl for a tumor with a diameter of 2 mm.

Whereas tumors originated from SKOV3-TR (CR) cells did not properly respond to paclitaxel (10 mg/kg) that was delivered twice a week for 2 weeks, injection of the anti-DX2 siRNA suppressed the growth rate of tumors over time (Figure 3B and D). In the case of A2780-CP20 (CR) cells, anti-DX2 siRNA treatment of three times displayed a decline in the tumor growth by 50%, while cisplatin (50 ml/kg) barely repressed the tumor growth (Figure 3C and E). We further confirmed the effect of the siRNA effect by measuring the volume and weight of the tumors that were isolated after the experiments (Figure 3F and G).

*Working mechanism of AIMP2-DX2 in TNF-α signaling*

AIMP2-F induces the TNF-induced cell death through the down-regulation of TNF receptor-associated factor 2 (TRAF2) that plays a

pivotal role in the TNF-α signaling pathway (Lee et al., 1997; Tada et al., 2001; Xiao, 2004; Xia and Chen, 2005). We thus investigated how AIMP2-DX2 would affect the activity of AIMP2-F in the regulation of TNF-α. To see whether AIMP2-DX2 would directly interact with TRAF2 as AIMP-F, we prepared GST-AIMP2-F and -DX2 proteins and mixed each protein with TRAF2 that was synthesized *in vitro*. TRAF2 was precipitated with both GST-AIMP2-F and -DX2 with similar affinity (Figure 4A). It was not surprising since the peptide region of AIMP2 spanning aa 84–225, that is still retained in AIMP2-DX2, was previously shown to be responsible for the interaction with TRAF2 (Choi et al., 2011). On the contrary, AIMP2-DX2 lost the ability to bind with KRS that is known to be the interacting partner within MSC (Choi et al., 2011) as shown by yeast two hybrids (Figure 4B). When the 293 cells were treated with TNF-α, the bindings of AIMP2-DX2 and -F to TRAF2 were both increased in a time-dependent manner (Figure 4C, right panel). To understand how AIMP2-DX2 compromises the apoptotic activity of TNF-α signaling, we checked whether AIMP2-DX2 would compete with AIMP2-F for the interaction with TRAF2. We transfected a different amount of AIMP2-DX2 and checked how it would affect the interaction of AIMP2-F and TRAF2 by co-immunoprecipitation. As the expression of AIMP2-DX2 was

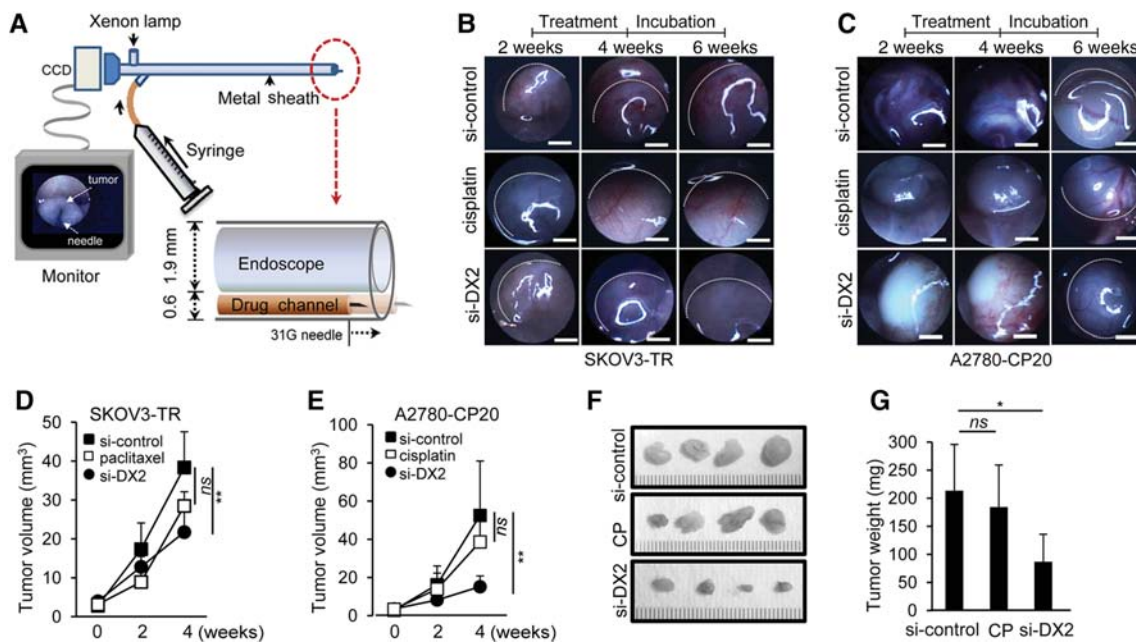


**Figure 3** The suppression of AIMP2-DX2 expression *in vivo*. (A) To get *in vivo* tumor imaging, laparoscope consisting of rigid telescope from Karl Storz was utilized. A 155 W xenon lamp for illumination was used as a light source and acquired images were recorded by CCD. A channel for drug delivery beside the endoscope channel was added. A thin stainless steel sheath (800  $\mu\text{m}$  in diameter) combined with the 31-G needle tip was connected with a 1 ml syringe. After putting it into the rigid telescope metal sheath (i.e. endoscope) together, the position of needle was controlled. Once the tumor site was observed, the drug channel was moved forward up to 1 mm. The mixture of siRNA and G-PEI could be introduced into the tumor (lower left figure). (B) SKOV3-TR cells were injected into abdomen of the nude mice. After 2 weeks, the first photo was taken by using specifically designed laparoscopy. siRNA or paclitaxel was treated twice a week repeatedly for another 2 weeks. Then the second photos were taken at 4 weeks from the implantation of tumor cells. After incubation of another 2 weeks, the last photos were prepared (indicated as 6 weeks). Scale bar, 2 mm. (C) A2780-CP20 cells were tested in the same way. (D and E) The growth curves of tumors derived from SKOV3-TR (D) and A2780-CP20 (E) cells were represented. Each experimental group contained six tumors from two animals. ns, not significant.  $**P < 0.01$ . (F) After finishing the experiment, six tumors from each group were isolated. Four representatives from each group were shown. (G) The weight of tumors was measured. ns, not significant;  $*P < 0.05$ .

increased, the interaction of AIMP2-F with TRAF2 was decreased (Figure 4D, left panel). Conversely, the introduction of AIMP2-F inhibited the interaction of AIMP2-DX2 with TRAF2 in a dose-dependent manner (Figure 4D, right panel). We confirmed these results by the *in vitro* pull-down assay using synthesized peptides. When we put different amounts of AIMP2-DX2 into the mixture of TRAF2 and AIMP2-F *in vitro*, the portion of AIMP2-F bound to TRAF2 was decreased according to the added amount of AIMP2-DX2 (Figure 4E, left panel). In reverse, as AIMP2-F was added in an increasing amount, AIMP2-DX2 interacting with TRAF2 was decreased (Figure 4E, right panel). Combined together, AIMP2-DX2 appears to compromise the function of AIMP2-F in the TNF- $\alpha$  signaling pathway through the competitive binding to TRAF2.

The E3 ubiquitin ligase, c-IAP1, was determined to be responsible for the AIMP2-dependent downregulation of TRAF2 (Choi et al., 2009a). Since AIMP2-DX2 can bind to TRAF2, we checked whether it can also bind c-IAP1. Flag-c-IAP1 was transfected with Myc-AIMP2-DX2, immunoprecipitated with anti-Flag antibody, and co-precipitation of AIMP2-DX2 was determined by western blotting with anti-Myc antibody. AIMP2-F was compared in parallel. While both proteins were expressed at a similar level, only AIMP2-F, not -DX2, was co-precipitated with c-IAP1 (Figure 4F), indicating that AIMP2-DX2 is not capable of binding

to c-IAP1. This possibility was further examined using *in vitro* pull-down assays. First, AIMP2-F and -DX2 were prepared by *in vitro* translation in the presence of [ $^{35}\text{S}$ ]methionine and mixed with GST or GST-c-IAP1. The GST proteins were pulled down with glutathione-Sepharose beads and the bound proteins were detected by autoradiography. AIMP2-F, but not from -DX2, was co-precipitated with GST-c-IAP1 while neither of them bound to GST (Figure 4G). Conversely, c-IAP1 was prepared by *in vitro* translation in the presence of [ $^{35}\text{S}$ ]methionine and mixed with GST-AIMP2-F or -DX2. GST-AIMP2-F or -DX2 was precipitated with glutathione-Sepharose and co-precipitation of c-IAP1 was detected by autoradiography. Again, c-IAP1 was detected only from the precipitate of GST-AIMP2-F, but not -DX2 (Figure 4H). Both results further support that AIMP2-DX2 cannot mediate the delivery of c-IAP1 to TRAF2 due to its incapability of interacting with c-IAP1.

#### *AIMP2-DX2 compromises the effect of AIMP2-F on TRAF2*

The results above suggest that AIMP2-DX2 would inhibit the pro-apoptotic interaction of AIMP2-F via TRAF2. We thus investigated how AIMP2-DX2 would affect the cellular level of TRAF2 upon TNF- $\alpha$  signaling. AIMP2-F significantly suppressed the TRAF2 level in the presence of TNF- $\alpha$  as previously reported (Figure 5A, left and middle panels). In contrast to AIMP2-F, the TNF- $\alpha$ -dependent suppressive effect was not observed in

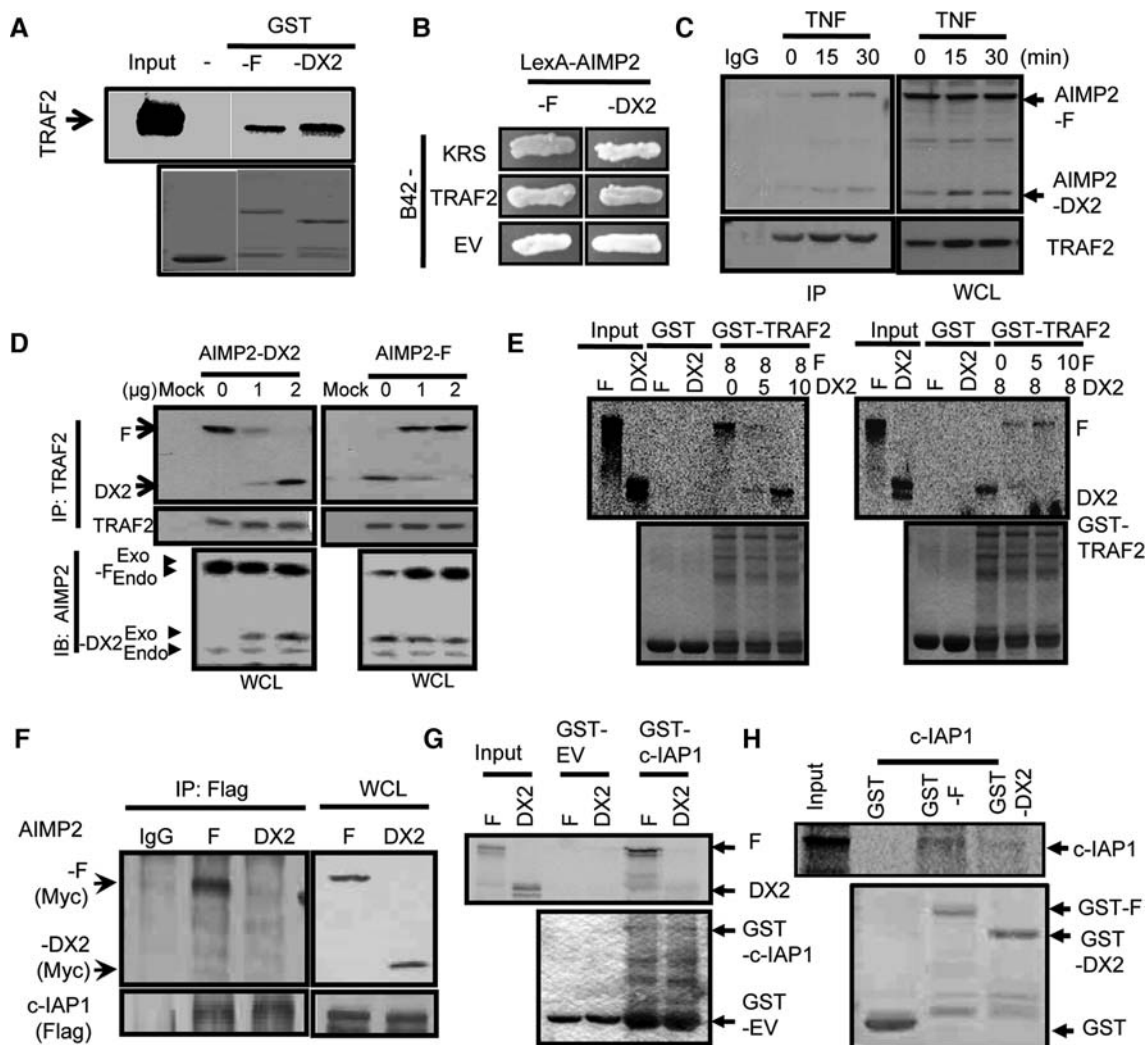


**Figure 4** Competition of AIMP2-DX2 for the interaction of AIMP2-F with TRAF2. (A) AIMP2-F and -DX2 were expressed as GST fusion proteins. TRAF2 was synthesized by *in vitro* translation and mixed with each of GST, GST-AIMP2-F, or -DX2, and precipitated with glutathione-Sepharose. Both the GST-AIMP2-F and -DX2, but not GST, were co-precipitated with TRAF2. (B) The interaction of LexA-AIMP2-F and -DX2 with B42-KRS and -TRAF2 was tested by the formation of blue colony on the X-gal plate using the yeast two-hybrid assay. The two forms of AIMP2 were expressed as B42 fusion proteins, and their interactions with TRAF2 or KRS that was expressed as the LexA fusion protein were tested by the yeast two-hybrid method. (C) Upon treatment of TNF- $\alpha$ , the interaction of AIMP2-F and -DX2 with TRAF2 was determined by co-immunoprecipitation at the indicated times. The extracted proteins were immunoprecipitated with anti-TRAF2 antibody and co-precipitated AIMP2-F and -DX2 were determined by western blotting with anti-AIMP2 antibody. (D) HEK293 cells were transfected with the indicated amount of Myc-AIMP2-DX2 and -F. The expression of endo- and exo-AIMP2-F and -DX2 was confirmed by western blotting of whole cell lysates (WCL) with anti-AIMP2 antibody (lower panel). TRAF2 was immunoprecipitated with its specific antibody and exo-AIMP2-F and -DX2 were detected with anti-Myc antibody (upper panel). (E) Radioactively synthesized AIMP2-F and -DX2 as above were used to see the pattern of interaction with TRAF2. The indicated amount of AIMP2-DX2 (indicated by microliter volume) was mixed with the fixed amount of AIMP2-F and GST-TRAF2 to see the effect of AIMP2-DX2 on the AIMP2-F binding to TRAF2. Conversely, the indicated amount of AIMP2-F was added to the fixed amount of AIMP2-DX2. (F) Flag-c-IAP1 was transfected into 293 cells with either Myc-AIMP2-F or -DX2. Flag-c-IAP1 was immunoprecipitated with anti-Flag antibody and co-immunoprecipitation of Myc-AIMP2-F or -DX2 was determined by western blotting with anti-Myc antibody. (G) AIMP2-F and -DX2 were prepared by *in vitro* translation in the presence of [ $^{35}$ S]methionine, mixed with either GST or GST-c-IAP1, precipitated with glutathione-Sepharose. AIMP2 proteins co-precipitated with GST or GST-c-IAP1 were detected by autoradiography. (H) AIMP2-F and -DX2 were expressed as GST fusion proteins, mixed with [ $^{35}$ S]methionine-labeled c-IAP1, and precipitated with glutathione-Sepharose. c-IAP1 co-precipitated GST proteins were detected by autoradiography.

AIMP2-DX2 (Figure 5A, right panel). We then compared the effect of AIMP2-F and -DX2 on the nuclear localization of NF- $\kappa$ B (p65) that is known to be induced by TNF- $\alpha$ . AIMP2-F suppressed the TNF- $\alpha$ -induced nuclear localization of NF- $\kappa$ B, whereas AIMP2-DX2 gave the opposite effect (Figure 5B, middle and right

panels, respectively). Considering that the opposite functions of AIMP2-F and -DX2 in the regulation of TRAF2 level, we examined the levels of TRAF2 in the tissue samples that were isolated from the mice after the *in vivo* anti-tumor effect test above (Figure 3). The level of TRAF2 in the isolated tumors was assessed by

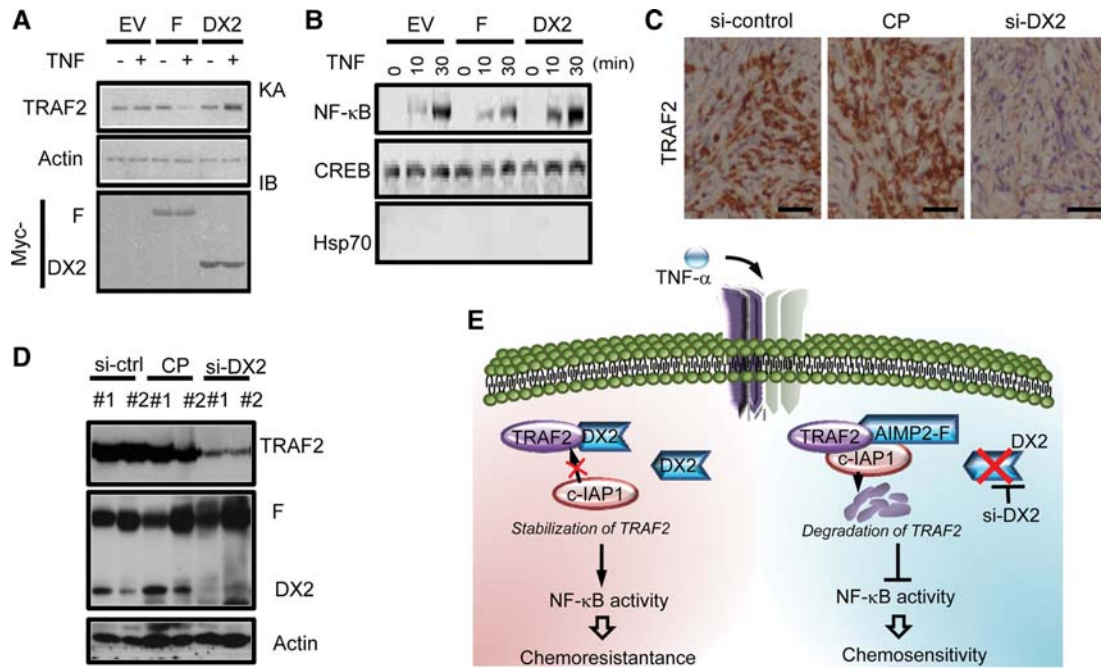


**Figure 5** AIMP2-F and -DX2 regulate the stability of TRAF2 in the dual pathway. **(A)** 293 cells were transfected with Myc-AIMP2-F or -DX2, and treated with TNF- $\alpha$  (30 ng/ml). The change in the TRAF2 level by the transfection of AIMP2-F and -DX2 was determined by western blotting with anti-TRAF2 antibody. Actin was used for loading control. Myc-tagged AIMP2-F and -DX2 were indicated (lower panel). **(B)** 293 cells were treated with TNF- $\alpha$ , harvested at the indicated times, and nuclear and cytosolic fractions were obtained to monitor the effect of AIMP2-F or -DX2 on the TNF- $\alpha$ -induced nuclear localization of NF- $\kappa$ B. CREB was used as a loading control of nuclear fraction and Hsp70 was checked to rule out the contamination from cytosolic fraction. **(C)** The isolated tumors from experiment in Figure 2 were fixed with 10% formalin and subjected to immunohistochemistry staining by TRAF2 antibody. Scale bar, 50  $\mu$ m. **(D)** The pattern of AIMP2-DX2 and TRAF2 expression repressed by si-AIMP2-DX2 was confirmed with the tissue samples by using western blotting. **(E)** In the condition of high AIMP2-DX2, pro-apoptotic function of AIMP2-F is compromised. TRAF2 can be stabilized, leading to aberrant activation of NF- $\kappa$ B. This environment elicits chemoresistance (left). When AIMP2-DX2 is downregulated by siRNA, the degradation of TRAF2 by facilitating the association of c-IAP1 with TRAF2 is induced, leading to downregulation of NF- $\kappa$ B activity (right).

immunohistochemical staining and western blotting with its specific antibody. As expected, TRAF2 levels were significantly reduced by the suppression of AIMP2-DX2 in both assays (Figure 5C and D). These results further confirm that AIMP2-DX2 compromises the function of AIMP2-F in TNF-induced TRAF2 degradation. Combined together, cancer cells appear to obtain a profit for chemoresistance by the increased expression of AIMP2-DX2 that would titrate pro-apoptotic function of normal full-length AIMP2 (Figure 5E, left panel) and the suppression of AIMP2-DX2 can control the survival of CR cells (Figure 5E, right panel).

## Discussion

Although chemoresistance in several types of cancer is often coupled directly or indirectly to the NF- $\kappa$ B activity, it is not simple to target NF- $\kappa$ B to restore chemosensitivity because direct suppression of NF- $\kappa$ B may give adverse effect on normal cells as well. Nevertheless, when the NF- $\kappa$ B activity is suppressed in CR cells, TNF- $\alpha$ -induced proliferation could be controlled (Wang et al., 1999). At this point of view, if there is a gene in the upstream of NF- $\kappa$ B signaling pathway that is expressed in association with cancer, it could be an alternative target for the control of CR cancer. We previously showed that AIMP2 augmented TNF- $\alpha$ -induced death through the ubiquitin-dependent degradation of TRAF2 (Choi

et al., 2009a). In this work, we demonstrated that the pro-apoptotic activity of AIMP2 via TRAF2 is compromised by the expression of its splicing variant lacking exon 2, AIMP2-DX2. Interestingly, the variant is highly expressed in the cancer region of the lung (Choi et al., 2011) and the ovary (Figure 1). Although this deleted form seems to be associated with p53 activation in lung cancer, the increased AIMP2-DX2 appears to affect the NF- $\kappa$ B activity more significantly rather than p53, at least in the case of ovarian cancer.

Alternative splicing is a key mechanism for the pathology of various diseases (Tazi et al., 2009). The splicing variants can exert the antagonistic or cooperative activities with respect to the function of the main expression form. Thus, it is considered as a fine tuning mechanism of cellular physiology to regulate the critical pathway. In the pathway of NF- $\kappa$ B regulation, several kinds of splicing variants associated with receptors and signal mediators have been identified in the upstream of NF- $\kappa$ B (Leeman and Gilmore, 2008). Here we report that the splicing variant of AIMP2, designated AIMP2-DX2, control the stability of TRAF2, weakening TNF- $\alpha$ -induced cell death.

In terms of chemoresistance, genotoxic stress of chemotherapy for ovarian cancer may activate NF- $\kappa$ B signaling (Janssens et al., 2005). Upon DNA damage, the p53-inducible death-domain containing protein elicits NF- $\kappa$ B activation through the regulation of

NEMO and RIP1. It was also reported that AIMP2 activates p53 under DNA damage condition. Therefore, AIMP2 might play as a mediator between p53 and NF- $\kappa$ B. To make the action mode of AIMP2-DX2 clear, we excluded the function of AIMP2-DX2 on p53 activation in this paper. However, *in vivo* conditions in which the tumors still express the wild type p53, AIMP2-DX2 might make CR cells more insensitive to chemotherapy by suppressing p53 and activating NF- $\kappa$ B simultaneously. Simultaneously targeting p53 and NF- $\kappa$ B pathway is thought to be a promising therapeutics to impair the aggressiveness of cancer cell (Dey et al., 2008; Ak and Levine, 2010). Thus, chemicals attacking the common pathway related to both molecules have been developed for cancer therapy (Dey et al., 2008). In this regard, AIMP2-DX2 could be an effective target to achieve this goal.

If AIMP2-DX2 is to block the pro-apoptotic activity of AIMP2-F, it may need to be present at the level that is stoichiometrically comparable with that of AIMP2-F. In this regard, it is worth noting that AIMP2-DX2 does not bind with KRS that is the component enzyme for MSC, whereas AIMP2-F strongly interacts with this enzyme (Choi et al., 2011) (Figure 4B). For this reason, AIMP2-DX2 is likely to exist separated from MSC, while AIMP2-F would mainly stay bound to the complex as shown before (Choi et al., 2011). Thus, AIMP2-DX2 could be more accessible to TRAF2 and effectively compete with AIMP2-F for the interaction with TRAF2 even if its total amount is much less than AIMP2-F.

Considering the increased AIMP2-DX2 level in CR cells, AIMP2-DX2 seems to confer benefit for cells to survive under the stress of chemotherapy. In the line of same logic, chemoresistant cancer cells would more heavily depend on AIMP2-DX2 for their survival. The data we obtained in this work suggest that AIMP2-DX2 can be employed as an adjunct therapeutic target for CR ovarian cancer. Since AIMP2-DX2 lost one of the functional domains, it would not be easy to design a drug that can specifically bind to AIMP2-DX2 but not -F. Instead, the AIMP2-DX2-specific siRNA can be formulated for the efficient delivery to the target cells. Alternatively, chemical drugs can be screened or designed to modulate the alternative splicing process to reduce the generation of AIMP2-DX2 or to induce the degradation of AIMP2-DX2 transcript.

## Materials and methods

### Cell lines and reagents

Human ovarian cancer cell lines A2780, SKOV3, and HeyA8 were purchased from ATCC. A2780-CP20, SKOV3-TR, and HeyA8-MDR were given from Dr Anil K. Sood of MD Anderson Cancer Center (USA). They were cultured in RPMI-1649 (Hyclone) including 10% fetal bovine serum (FBS) and gentamycin (250 ng/ml). SKOV3-TR and HeyA8-MDR were supplemented with 150 and 300 ng/ml of paclitaxel, respectively, to preserve their CR property. The 293 cells were cultivated in Dulbecco's modified Eagle's medium (DMEM) supplemented with 10% FBS and 50  $\mu$ g/ml penicillin and streptomycin in a 5% CO<sub>2</sub> incubator. Myc- and Flag-tagged TRAF2 were kindly provided by S.Y. Lee (Ewha Womans University, Korea). The wild type and K48R or K63R mutant ubiquitin clones were kind gifts from C.H. Jung (Seoul National University, Korea). Geneporter (GTS) and lipofectamine 2000 (Invitrogen) were used as transfection reagents.

Human TNF- $\alpha$  (Sigma) was treated at the various concentrations (20–40 ng/ml) according to experimental purpose. MG-132 (Calbiochem) was added at the concentration of 20  $\mu$ M in serum-free condition. The siRNAs of AGAGCUUGCAGAGACAGGUUAGACU and UCAGCGCCCGUAAUCCUGCAGGUG specifically targeting AIMP-F and -DX2, respectively, were designed as described previously (Choi et al., 2011) and obtained from Invitrogen. Stealth universal RNAi (Invitrogen) was used as the non-specific control. The cDNAs encoding mouse forms of AIMP2-F and -DX2 were obtained by RT-PCR and cloned to pcDNA 3.1(+) plasmid using *Hind*III and *Xho*I sites.

### Tumor samples

This study was approved by the Institutional Review board of Samsung Medical Center (SMC 2009-09-002-002). We obtained fresh frozen tumor specimens from the primary ovary during surgery from women with epithelial ovarian cancer ( $n = 40$ ). As controls, we also obtained normal ovarian tissues ( $n = 11$ ) from women who underwent hysterectomies for benign disease. All operations were performed by the Department of Obstetrics and Gynecology at the Samsung Medical Center between October 2003 and November 2005. All women with cancer underwent primary maximal cytoreductive surgery followed by intravenous paclitaxel (175 mg/m<sup>2</sup>) or docetaxel (75 mg/m<sup>2</sup>) plus carboplatin (AUC 5) combination chemotherapy every 3 weeks for six to eight cycles. Patients were divided into two groups according to the sensitivity for first-line platinum-based combination chemotherapy. CR is defined as the platinum-free interval <6 months. Surgical staging was established according to the International Federation of Gynecology and Obstetrics system (Supplementary Table S2).

### Real-time PCR

After cell lysis with Trizol<sup>TM</sup> (Invitrogen), the cell extracts were incubated with 50% chloroform. After vortexing, the mixtures were centrifuged at 14000 rpm at 4°C. The upper layers were collected and isopropanol was added for RNA precipitation. After washing with 70% ethanol, 1  $\mu$ g of RNA dissolved in the distilled water was used as the template for PCR with the sets of primers. The sequences of forward primer for AIMP2-F and -DX2 are ACCGGCTCCCAACGTGCAC and CTGGCCACGTGCAGGATTACGG GG, respectively. The backward primer AAGTGAATCCCAGCT GATAG was used for both AIMP2-F and -DX2. To normalize the expression, PAPOLA gene was used as described previously (Choi et al., 2011). The sequences of the primers were GCGAGGTCCT CACTCAGC and TTCTTTCTCAATTAGAATGTCAATGC. The Taqman probes were provided from Applied Biosystem (Life Technology), and PCR was performed through the cycle of 10 sec at 95°C, 20 sec at 60°C, and 5 sec at 72°C.

### Western blot analysis

To analyze the tissue distribution of AIMP2-F and -DX2, we homogenized different mouse organs in the lysis buffer containing 1% Triton X-100, 0.1% SDS, and protease inhibitor cocktail. The cultivated cells lines were dissolved in the lysis buffer containing 0.5% Triton X-100 and protease inhibitor cocktail. The proteins extracted from the homogenized cells and cell lines were separated by 10% SDS-PAGE. To isolate nuclear fractions, we used ProteoExtract kit (Calbiochem) following the manufacturer's instruction.

### Flow cytometry

Cells transfected with the plasmid encoding AIMP2-F or -DX2 were cultivated in the absence or presence of TNF- $\alpha$  (40 ng/ml) or UV (50 J/m<sup>2</sup>) for 24 h, fixed with 70% ethanol for 1 h at 4°C and washed with ice-cold PBS two times. Then,  $1 \times 10^6$  cells were stained with PI (50  $\mu$ g/ml PI, 0.1% sodium citrate, 0.3% NP-40, and 50  $\mu$ g/ml RNase A) for 40 min and subjected to FACS Calibur flow cytometry (Beckton-Dickinson) for the determination of apoptotic cells by counting sub-G1 cells and annexin V staining following manufacturer's instruction (Invitrogen). All of the experiments were repeated three times and averaged.

### Colony-forming assay

For soft agar colony assays, cells were diluted into 0.3% agar in DMEM containing 20% FBS and seeded in triplicate onto solidified 0.6% agar containing the culture medium of 500  $\mu$ l per 15 mm plate. The colonies were fed every 3–4 days and evaluated after 4 weeks. Another group was also cultivated in the presence of TNF- $\alpha$  (30 ng/ml) under the same condition. The colony formation was then visualized and counted by Coomassie blue staining.

### Co-immunoprecipitation

The cultivated cells were dissolved in the lysis buffer containing 0.5% Triton X-100 and protease inhibitor cocktail, and the lysates were centrifuged at 14000 rpm for 30 min. We then separated the extracted proteins by SDS-PAGE. To examine the interaction of AIMP2-F or -DX2 with TRAF2, the cells were lysed with the immunoprecipitation (IP) lysis buffer (20 mM Tris-HCl, pH 7.4, 150 mM NaCl, and 0.2% NP-40). The protein extracts were incubated with normal IgG and protein G agarose for 2 h, and then centrifuged to remove non-specific IgG binding proteins. We then mixed the supernatant with the TRAF2 antibody (Santa Cruz), incubated for 2 h at 4°C with agitation and added protein G agarose. After washing three times with ice-cold lysis buffer, the precipitates were dissolved in the SDS sample buffer and separated by SDS-PAGE. To detect AIMP2, we used a 10% SDS-PAGE gel. After the proteins were transferred to PVDF membrane, co-immunoprecipitation of AIMP2-F or -DX2 was determined with the anti-AIMP2 antibody.

### Yeast two-hybrid assay

AIMP2-F and -DX2 were cloned to both pLexA and pB42 vectors. The full-length TRAF2 was ligated to the pLexA and pB42 vectors at *Eco*RI and *Xho*I sites. The positive interactions were determined by the formation of blue colonies on the X-gal-containing yeast medium as described previously (Rho et al., 1999).

### GST-pull down

We expressed GST-AIMP2 or GST in *Escherichia coli* Rosetta (DE3) strain and mixed the protein extracts containing GST-AIMP2 or GST with glutathione-Sepharose in the PBS buffer containing 1% Triton X-100 and 0.5% *N*-laurylsarcosine at 4°C for 2 h. We synthesized human TRAF2 by *in vitro* translation in the presence of [<sup>35</sup>S]methionine using pcDNA3.1/V5-His-TOPO-AIMP2 (or -DX2) as the template, added to the GST protein mixtures, incubated at 4°C for 6 h with rotation in the PBS buffer containing 1% Triton X-100, 0.5% *N*-laurylsarcosine, 1 mM DTT, 2 mM EDTA, and 300  $\mu$ M phenylmethylsulfonyl fluoride, and washed six times with the same buffer containing 0.5% Triton X-100. We then eluted the proteins bound to Sepharose beads with the SDS sample buffer, separated by SDS-PAGE and determined AIMP2 by

autoradiography. Similarly, the interaction of c-IAP1 with AIMP2-F or -DX2 was determined using GST-c-IAP1 with radioactively synthesized AIMP2-F and -DX2. The trimeric interaction between TRAF2 with c-IAP1 and AIMP2 was also examined by the *in vitro* pull-down assay. We expressed GST-TRAF2 in *E. coli* Rosetta (DE3) and mixed the protein extracts with glutathione-Sepharose in the PBS buffer containing 1% Triton X-100 and 0.5% *N*-laurylsarcosine at 4°C for 2 h. Then, *in vitro* synthesized c-IAP1 and AIMP2-F were then added to the GST protein mixtures, incubated at 4°C for 6 h with rotation in the PBS buffer containing 1% Triton X-100, 0.5% *N*-laurylsarcosine, 1 mM DTT, 2 mM EDTA, and 300  $\mu$ M phenylmethylsulfonyl fluoride, and washed six times with the same buffer containing 0.5% Triton X-100. GST-TRAF2 and -c-IAP1 were the kind gifts from Dr Ze'ev Ronai (Burnham Institute, USA) and Dr J. Ashwell (NIH, USA), respectively.

### Reporter gene assay

To test the NF- $\kappa$ B-dependent transcriptional activity, NF- $\kappa$ B-luciferase vector (kindly provided by Dr Jonathan Ashwell, NIH, USA) was co-transfected into SKOV3, SKOV3-TR, A2780, and A2780-CP20 cells with pcDNA3.1 empty vector and the cells were selected by G418 (1 mg/ml) for 1 week to establish the stable expressing cells. After the selection of cells survived, we subsequently introduced the empty vector (as the control), AIMP2-F or -DX2 into the cells, and treated TNF- $\alpha$  (20 ng/ml) for 12 h. The cell lysates were prepared and reacted by the luciferase assay kit following the manufacturer's protocol (Promega) and the luciferase activity was analyzed by using luminometer.

### Laparoscopy and *in vivo* siRNA injection

The animal study was approved by Institutional Animal Care and Use Committee of the Samsung Medical Center (C-B0-224-2). A laparoscopy containing two channels of microneedle and microscope was designed. Both CS and CR cells of SKOV3 and A2780 cells were injected intraperitoneally at the number of  $1 \times 10^6$ . Then they were incubated for tumor formation for 2 weeks. After being injected the mixture of 80 mg/kg ketamine and 10 mg/kg xylazine, the anesthetized mouse was put on a temperature-regulated plate of the microscope stage to keep them warm. The tissue beneath including the fascia, peritoneal muscles, and peritoneum was incised carefully, at the size of 5 mm, to access the internal organs on both sides of the abdomen. The endoscope was introduced into the abdominal cavity through this opening. To identify and monitor the same tumors from the beginning we selected the well isolated tumors and the locomotion path of laparoscopy from the incision was recorded in detail for each tumor. The location of tumors was confirmed by the structure of the surrounding tissues that were compared with those of the previous photos. Once the image of a tumor was taken in focus, we then got the image of a ruler in the same focus to calculate the size of tumor. The incision was closed by suture for repetitive imaging at later time point. Each experimental group consisted of six and three tumors from an animal were chosen. The photos were taken three times at the time interval of 2 weeks for each tumor and siRNA was introduced three times for the first 2 weeks. For siRNA delivery, 50  $\mu$ g of siRNA was mixed with GDM-PEI at 1.64:1 weight ratio in 0.9% saline. The complex was directly injected into tumors in two directions for four times in the indicated interval. The volume was calculated by (2 width  $\times$  height)/2.

### Statistical analysis

Statistical analysis was performed with SPSS for window version 15.0 (SPSS, Inc.). Each experiment was carried out at least three times in triplicate. The Pearson's chi-square and Fisher's exact tests were used to assess the statistical significance of the association between AIMP2-DX2 expression and clinicopathological parameters. The comparison of DX2 expression between the normal ovarian tissues and EOCs was performed using the Mann-Whitney test (for real-time RT-PCR analysis). Differences in cell survival rates as measured by the MTT assay were assessed by a two-sample *t*-test or two-way of ANOVA test.  $P < 0.05$  was considered of significant difference.

### Supplementary material

Supplementary material is available at *Journal of Molecular Cell Biology* online.

### Funding

This work was supported in part by the Global Frontier grant (NRF-M1AXA002-2010-0029785) of National Research Foundation (the Ministry of Education, Science, and Technology of Korea) and by the Korea Healthcare technology R&D project grant (A092255, the Ministry for Health & Welfare Affairs, Korea).

**Conflict of interest:** none declared.

### References

- Ak, P., and Levine, A.J. (2010). p53 and NF-kappaB: different strategies for responding to stress lead to a functional antagonism. *FASEB J.* 24, 3643–3652.
- Balkwill, F. (2006). TNF-alpha in promotion and progression of cancer. *Cancer Metastasis Rev.* 25, 409–416.
- Charles, K.A., Kulbe, H., Soper, R., et al. (2009). The tumor-promoting actions of TNF-alpha involve TNFR1 and IL-17 in ovarian cancer in mice and humans. *J. Clin. Invest.* 119, 3011–3023.
- Chen, R., Alvero, A.B., Silasi, D.A., et al. (2007). Inflammation, cancer and chemoresistance: taking advantage of the toll-like receptor signaling pathway. *Am. J. Reprod. Immunol.* 57, 93–107.
- Choi, J.W., Kim, D.G., Park, M.C., et al. (2009a). AIMP2 promotes TNFalpha-dependent apoptosis via ubiquitin-mediated degradation of TRAF2. *J. Cell Sci.* 122, 2710–2715.
- Choi, J.W., Um, J.Y., Kundu, J.K., et al. (2009b). Multidirectional tumor-suppressive activity of AIMP2/p38 and the enhanced susceptibility of AIMP2 heterozygous mice to carcinogenesis. *Carcinogenesis* 30, 1638–1644.
- Choi, J.W., Kim, D.G., Lee, A.E., et al. (2011). Cancer-associated splicing variant of tumor suppressor AIMP2/p38: pathological implication in tumorigenesis. *PLoS Genet.* 7, e1001351.
- Dey, A., Tergaonkar, V., and Lane, D.P. (2008). Double-edged swords as cancer therapeutics: simultaneously targeting p53 and NF-kappaB pathways. *Nat. Rev. Drug Discov.* 7, 1031–1040.
- Dobrzycka, B., Terlikowski, S.J., Garbowski, M., et al. (2009). Tumor necrosis factor-alpha and its receptors in epithelial ovarian cancer. *Folia Histochem. Cytobiol.* 47, 609–613.
- Eltabbakh, G.H. (2004). Recent advances in the management of women with ovarian cancer. *Minerva Ginecol.* 56, 81–89.
- Han, J.M., Park, B.J., Park, S.G., et al. (2008). AIMP2/p38, the scaffold for the multi-tRNA synthetase complex, responds to genotoxic stresses via p53. *Proc. Natl Acad. Sci. USA* 105, 11206–11211.
- Hernandez, L., Hsu, S.C., Davidson, B., et al. (2010). Activation of NF-kappaB signaling by inhibitor of NF-kappaB kinase beta increases aggressiveness of ovarian cancer. *Cancer Res.* 70, 4005–4014.
- Hsu, H., Shu, H.B., Pan, M.G., et al. (1996). TRADD-TRAF2 and TRADD-FADD interactions define two distinct TNF receptor 1 signal transduction pathways. *Cell* 84, 299–308.
- Janssens, S., Tinel, A., Lippens, S., et al. (2005). PIDD mediates NF-kappaB activation in response to DNA damage. *Cell* 123, 1079–1092.
- Karin, M. (2006). Nuclear factor-kappaB in cancer development and progression. *Nature* 441, 431–436.
- Kim, M.J., Park, B.J., Kang, Y.S., et al. (2003). Downregulation of FUSE-binding protein and c-myc by tRNA synthetase cofactor p38 is required for lung cell differentiation. *Nat. Genet.* 34, 330–336.
- Kwong, J., Chan, F.L., Wong, K.K., et al. (2009). Inflammatory cytokine tumor necrosis factor alpha confers precancerous phenotype in an organoid model of normal human ovarian surface epithelial cells. *Neoplasia* 11, 529–541.
- Lee, S.Y., Reichlin, A., Santana, A., et al. (1997). TRAF2 is essential for JNK but not NF-kappaB activation and regulates lymphocyte proliferation and survival. *Immunity* 7, 703–713.
- Leeman, J.R., and Gilmore, T.D. (2008). Alternative splicing in the NF-kappaB signaling pathway. *Gene* 423, 97–107.
- Liu, Z.G. (2005). Molecular mechanism of TNF signaling and beyond. *Cell Res.* 15, 24–27.
- Liu, G.H., Wang, S.R., Wang, B., et al. (2006). Inhibition of nuclear factor-kappaB by an antioxidant enhances paclitaxel sensitivity in ovarian carcinoma cell line. *Int. J. Gynecol. Cancer* 16, 1777–1782.
- McGuire, W.P., Hoskins, W.J., Brady, M.F., et al. (1996). Cyclophosphamide and cisplatin compared with paclitaxel and cisplatin in patients with stage III and stage IV ovarian cancer. *N. Engl. J. Med.* 334, 1–6.
- Micheau, O., and Tschopp, J. (2003). Induction of TNF receptor I-mediated apoptosis via two sequential signaling complexes. *Cell* 114, 181–190.
- Nakanishi, C., and Toi, M. (2005). Nuclear factor-kappaB inhibitors as sensitizers to anticancer drugs. *Nat. Rev. Cancer* 5, 297–309.
- Rho, S.B., Kim, M.J., Lee, J.S., et al. (1999). Genetic dissection of protein-protein interactions in multi-tRNA synthetase complex. *Proc. Natl Acad. Sci. USA* 96, 4488–4493.
- Sethi, G., Sung, B., Kunnumakkara, A.B., et al. (2009). Targeting TNF for treatment of cancer and autoimmunity. *Adv. Exp. Med. Biol.* 647, 37–51.
- Sood, A.K., and Buller, R.E. (1998). Drug resistance in ovarian cancer: from the laboratory to the clinic. *Obstet. Gynecol.* 92, 312–319.
- Tada, K., Okazaki, T., Sakon, S., et al. (2001). Critical roles of TRAF2 and TRAF5 in tumor necrosis factor-induced NF-kappa B activation and protection from cell death. *J. Biol. Chem.* 276, 36530–36534.
- Tazi, J., Bakkour, N., and Stamm, S. (2009). Alternative splicing and disease. *Biochim. Biophys. Acta* 1792, 14–26.
- Wang, C.Y., Cusack, J.C., Jr., Liu, R., et al. (1999). Control of inducible chemoresistance: enhanced anti-tumor therapy through increased apoptosis by inhibition of NF-kappaB. *Nat. Med.* 5, 412–417.
- Xia, Z.P., and Chen, Z.J. (2005). TRAF2: a double-edged sword? *Sci. STKE* 2005, pe7.
- Xiao, W. (2004). Advances in NF-kappaB signaling transduction and transcription. *Cell Mol. Immunol.* 1, 425–435.